



ELSEVIER

Physica C 227 (1994) 259–266

PHYSICA C

Ca induced line defects and superconductivity in $Y_xSr_2Cu_2GaO_7$

J.P. Zhang^{a,b}, D.A. Groenke^{a,c}, B. Dabrowski^{a,d,e}, K.R. Poeppelmeier^{a,c},
L.D. Marks^{a,b,*}

^a Science and Technology Center for Superconductivity, Northwestern University, Evanston, IL 60208, USA

^b Department of Materials Science and Engineering, Northwestern University, Evanston, IL 60208, USA

^c Department of Chemistry, Northwestern University, Evanston, IL 60208, USA

^d Materials Science Division, Argonne National Laboratory, Argonne, IL 60439, USA

^e Department of Physics, Northern Illinois University, DeKalb, IL 60115, USA

Received 12 August 1993; revised manuscript received 25 April 1994

Abstract

The microstructure of Ca doped $Y_{1-x}Ca_xSr_2Cu_2GaO_7$ and Ca substituted $YSr_{2-x}Ca_xCu_2GaO_7$ have been investigated by electron microscopy. A common feature found in the $Y_{1-x}Ca_xSr_2Cu_2GaO_7$ superconductors is the existence of line defects, which are not observed in non-superconducting $YSr_{2-x}Ca_xCu_2GaO_7$. At the higher doping level, $x \approx 0.35$, the line defects develop into modulated structures. The transition temperature and Meissner fraction increases with the doping level as does the defect concentration, indicating that the defects and superconductivity in these materials are interrelated. The line defects are associated with an asymmetrical distortion ($a_p \neq b_p$) of the gallium–oxygen plane which plays a similar role to the copper–oxygen chains in $YBa_2Cu_3O_{7-\delta}$.

1. Introduction

An important issue in cuprate superconductors is how the local environment acts upon the two dimensional $Cu-O_2$ layer(s) in a superconducting structure. Among those systems discovered up to now, there are two common $Cu-O_2$ structures that have been observed:

(1) single $Cu-O_2$ sheets separated by AO layers, and
(2) paired sheets of $CuO_2-M-CuO_2$ intergrown with metal oxide layers. $La_{2-x}M_xCuO_4$ ($M = Ca, Sr, Ba$) [1] and $Nd_{2-x}Ce_xCuO_4$ [2] are examples of the first type and $Y-Ba-Cu-O$ [3], Bi [4] and Tl based [5] superconductors are of the second type. The new cuprate $YSr_2Cu_2GaO_7$ [6–8] has a $YBa_2Cu_3O_7$ (123)-like structure and exhibits superconductivity with cal-

cium substitution for yttrium. Because there is only one $CuO_2-Y-CuO_2$ unit and the gallium–oxygen plane has replaced the copper chain, any argument for charge transfer between the chains and planes does not exist. Therefore, detailed studies of microstructure and superconductivity in this new compound are of fundamental interest.

$Y_{1-x}Ca_xSr_2Cu_2GaO_7$ annealed in high oxygen pressure is superconducting at $x > 0.15$, and the transition temperature is found to increase with the doping level as well as the Meissner fraction, but the lattice parameters decrease as reported previously [9]. A transmission electron microscopy study confirmed that $YSr_2Cu_2GaO_7$ is a double triple-perovskite structure with $a \times b \times c = 6a_p \times \sqrt{2}a_p \times \sqrt{2}a_p$, space group $Ima2$, with the two gallium–oxygen planes placed non-centrosymmetrically in a unit cell as has been verified by

* Corresponding author.

high-resolution imaging [9]. $Y_{1-x}Ca_xSr_2Cu_2GaO_7$ samples were found to have the same average structure as $YSr_2Cu_2GaO_7$. When $x \geq 0.30$ ($Y_{1-x}Ca_xSr_2Cu_2GaO_7$), the presence of a second phase $Sr_{14-x}Ca_xCu_{24}O_{41}$ was found, approximately six percent in weight. No formation of a second phase of $YSr_2(Cu, Ga)_3O_7$ was detected [9].

In this study, we demonstrate, unique to the gallium superconductors, the existence of line defects along the c -axis of the material, not recognized by bulk techniques, which can be attributed to local changes in the structure of the gallium–oxide units. These were not found in non-superconducting $YSr_{2-x}Ca_xCu_2GaO_7$ processed under the same conditions. The density and morphology of these defects varies with doping level, and a link between defects and superconductivity of gallium superconductors will be discussed.

2. Experimental methods

Polycrystalline samples of $Y_{1-x}Ca_xSr_2Cu_2GaO_7$ ($x = 0.2, 0.25$ and 0.4) and $YSr_{2-x}Ca_xCu_2GaO_7$ ($x = 0.3, 0.4$) were synthesized from stoichiometric amounts of (Aldrich) Y_2O_3 (99.99%), $CaCO_3$ (99.995%), $SrCO_3$ (99.995%), CuO (99.99%), and Ga_2O_3 (99.99%) as described previously [9]. After preparation, all the samples were annealed under the same conditions: high-pressure oxygen (200–500 bar) at 910–970°C, followed by slow cooling at 2°C/min [9].

For the electron microscopy we have primarily used powder samples that were crushed and dispersed onto

holey carbon films. Electron diffraction patterns along different crystallographic directions (equivalent to single-crystal X-ray patterns) were obtained using a Hitachi H700 operated at 200 kV. High-resolution electron microscopy was performed using a Hitachi H9000 operated at 300 kV.

Susceptibility measurements were performed on a Quantum Design MPMS Squid Susceptometer operated between 4 and 300 K. The lattice parameters, the transition temperature, and the Meissner fraction as a function of the calcium concentration for the samples used for this study have been previously reported [9].

3. Results

3.1. Electron diffraction data

For all the compositions $Y_{1-x}Ca_xSr_2Cu_2GaO_7$ ($x = 0.2, 0.35$ and 0.4), streaks appeared in the reciprocal c planes, are shown in a [100] zone in Fig. 1(a). When the crystals were tilted along the c -axis, these streaks appeared in all zones, see Figs. 1(b) and (c). This implies that the streaks are planes in reciprocal space cut by the rather flat Ewald sphere. These reciprocal planes indicate linear features in real space, which are extended along [001] because of the sharpness of the streaks in the c^* direction. This has been verified by electron-diffraction examination for more than sixty $Y_{1-x}Ca_xSr_2Cu_2GaO_7$ crystals at different doping levels with $x > 0.15$. To be specific about the description of these features, they correlate to lines along [001] in real space and intersect in reciprocal space at $[00h + \delta]$

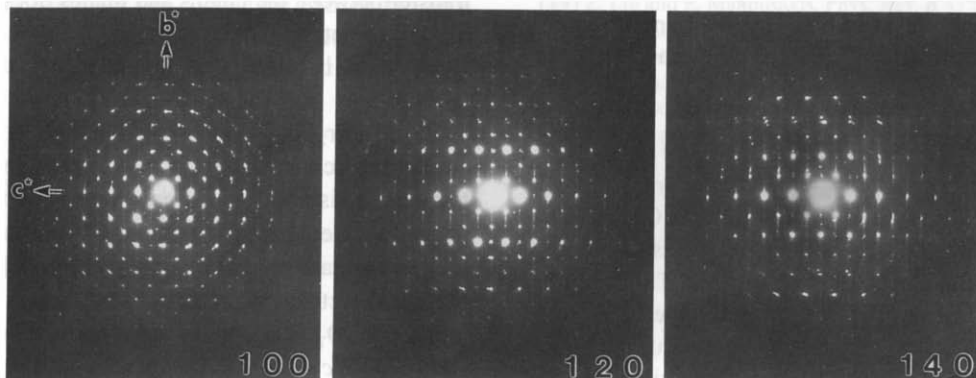


Fig. 1. Diffraction patterns from a single grain as a function of tilt angle. The streaks apparent along the b -axis show up as planes in reciprocal space, implying linear features in real space along the c -axis.

where δ is positive, zero, and δ varied experimentally.

The $Y_{1-x}Ca_xSr_2Cu_2GaO_7$ crystals were also examined along the directions perpendicular to the a -axis, and no streaks were observed in the $[001]$ zone. Along $[021]$, the streaks were found at $\frac{1}{2}g_{012}$ positions with appreciable intensities as shown in Fig. 2 (a). There are always some spots superimposed on the streaks which have the same periodicity as the matrix. This indicates that the defects are located in the structure, and the electron beam is dynamically diffracted when passing through the crystals by both the matrix and the defects. These streaks (or the extra spots on the streaks) are quite strong, implying that the line defects have a considerable number density. They are also stronger at

the higher doping levels, indicating higher densities. The position of streaks varies from $\frac{1}{2}g_{012}$ to $(\frac{1}{2} + \delta)g_{012}$, where δ is smaller than 2%, indicating the defective structure is incommensurate with the lattice. In contrast to $[021]$, for an untwinned $[012]$ zone (Fig. 2(b)) the streaks intersected the reciprocal lattice spots; with respect to the crystal symmetry the defects are strongly orthorhombic.

For $YSr_{2-x}Ca_xCu_2GaO_7$ ($x=0.3, 0.4$), more than forty crystals were examined and no streaks were found. For comparison, a $[021]$ pattern is presented in Fig. 2(c). In another non-superconducting gallium compound, an undoped $YSr_2Cu_2GaO_7$ and a $YCaSrCu_2GaO_7$ annealed under low oxygen pressure, the

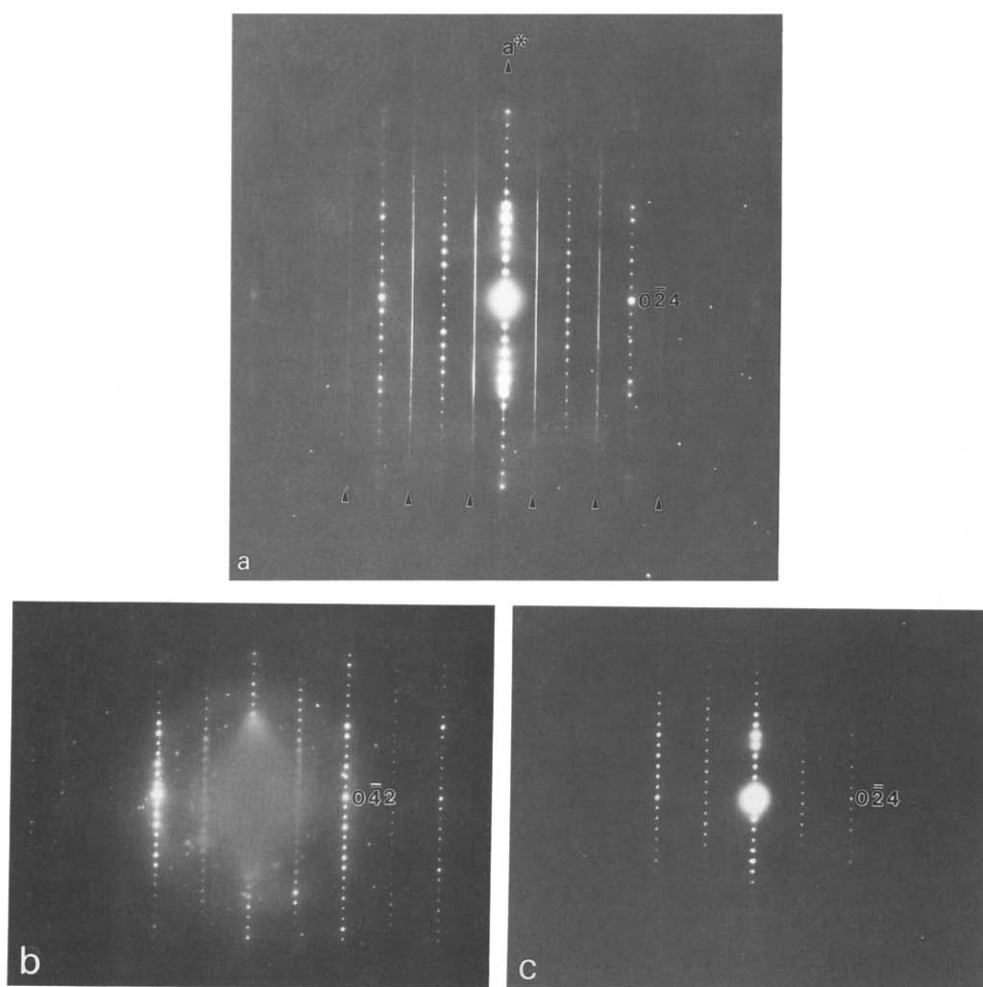


Fig. 2. The appearance of streaks at the $\frac{1}{2}g_{012}$'s positions can be observed in the $[021]$ zone from $Y_{0.6}Ca_{0.4}Sr_2Cu_2GaO_7$, shown in (a), but not in the $[012]$ zone in (b) or $[021]$ of $YSr_{1.6}Ca_{0.4}Cu_2GaO_7$, see (c).

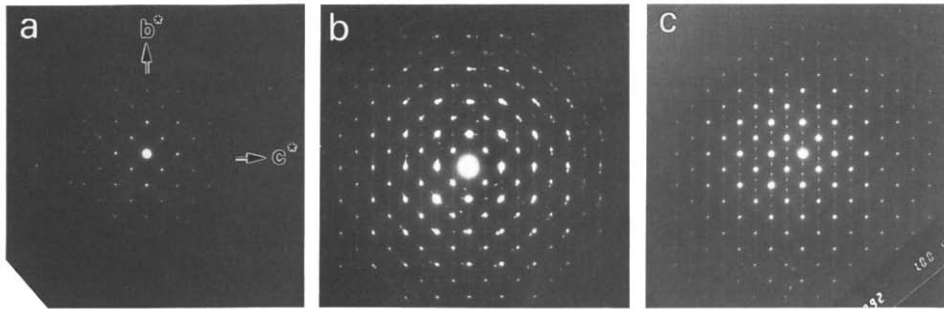


Fig. 3. [100] diffraction patterns showing how the intensities of the streaks vary as a function of calcium content in $Y_{1-x}Ca_xSr_2Cu_2GaO_7$: (a) $x=0$, (b) $x=0.2$, (c) $x=0.4$.

[021] patterns were clean, i.e. no streaks were observed. This indicates that the line defects are only found in gallium superconductors.

The intensities of the streaks varied as a function of the calcium content as shown in Fig. 3. At $x=0.35$, the streak intensity reached the highest level and extra spots occurred at the positions of $\frac{1}{3}$ and/or $\frac{1}{4}$ of g_{020} . There was no significant change in intensity when the doping level was higher, e.g. $x=0.4$. These extra spots indicate an ordering along the b direction, incommensurate with the lattice. We will refer to these later in the text as ‘‘tubes’’ since they have a definite width, as against the lines where there was little to no intensity variation along the streaks. Diffraction patterns taken from more than 30 different crystals along $[0vw]$ directions showed no extra features along $h00$. This indicates that planar defects or stacking faults of different M–O (M = Y, Ga, Sr or Cu) planes are not present in our material, different from the observation [10] of superstructures in non-superconducting $(Nd, Ce)_nO_{2n}Sr_2GaCu_2O_5$ and $YSr_2CoCu_2O_7$. (High-resolution images along [100], [010] and other $[0vw]$ zones confirm this conclusion).

3.2. High-resolution imaging

In the $Y_{1-x}Ca_xSr_2Cu_2GaO_7$ ($x=0.35$ and 0.4) samples, structural variants can be seen in [100] high-resolution images as shown in Fig. 4. The tube-like structures are along the c -axis through the whole grains with a width of 8.1 ($3 \times d_{020}$) or 11 Å ($4 \times d_{020}$) along the b direction. From the diffraction study, it is clear that the extra spots at $\frac{1}{3}$ or $\frac{1}{4}$ g_{020} are always associated with the streaks, and that the dimensions of the tubes viewed along [100] are compatible with the line fea-

tures observed in [001] images (see below). In order to obtain higher contrast, tilted illumination dark field imaging was applied along [100] because the individual line defects scatter weakly. The (high-resolution) dark-field images show both 8 Å and 11 Å tubes, see Fig. 5, which are straight along the b direction for at least 1000 Å [11].

In order to understand the unusual line features in this material, high-resolution imaging was employed along the c direction, directly down the line defects. As shown in Fig. 5, the intensities of the centers of some white circles are slightly different with the normal ones, and they change at different foci. The white circles are the SrO–GaO–SrO frames, verified by image simulations [9] and the [001] high-resolution images indicate a structure change in the gallium–oxygen planes.

To clarify the structure of these defects using experimental imaging and image simulations would require instrumentation well beyond what is currently available. However, we can make some quite definite statements about what they are not, and where they are in the structure. First, they are definitely in the GaO layers. Second, they are weak, so the most that they can correspond to is a rather small change in the structure. Attempts to simulate the high-resolution images of [001] $Y_{1-x}Ca_xSr_2Cu_2GaO_7$ structure with defects in the SrO–GaO–SrO layers were performed with different structure models, for example, the strontium, gallium and oxygen atoms arranged in a structure similar to $LaSrCuAlO_5$ [12] to form a 11 Å tube. The calculated results showed that images with a distortion in the strontium–oxygen planes do not match the experimental ones. One possibility is that we have very local twinning; except for the GaO layers the [010] and [001] zones in this material are almost identical. Image

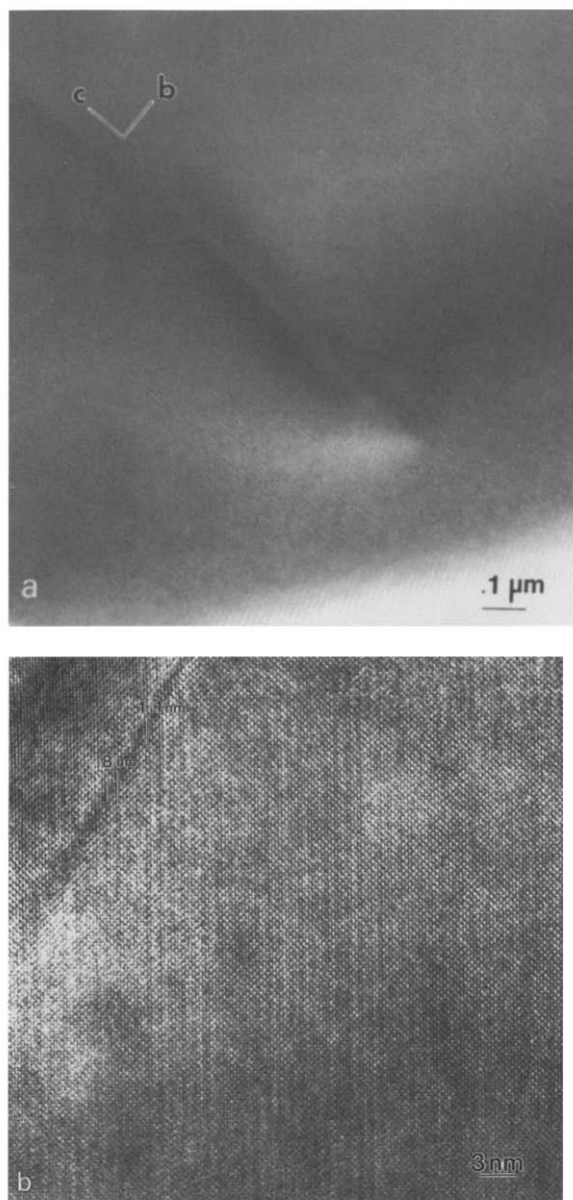


Fig. 4. High-resolution images from [100] crystals of $Y_{0.6}Ca_{0.4}Sr_2Cu_2GaO_7$: (a) bright field image showing the 8 Å and 11 Å tube-like defects; (b) dark-field image showing these defects are straight.

simulations using this type of model seemed to be reasonable, but we have far too little experimental information to work with to avoid ambiguities. For example, a full focal series was microdensitometered and analyzed digitally, but even then there was not sufficient

information for proper, and unique, through-focus through-thickness matching of the defects.

4. Discussion

Line defects appear to be the unique feature of the microstructure of the $Y_{1-x}Ca_xSr_2Cu_2GaO_7$ superconductors, and it is appropriate to look for correlations between the Meissner fraction, transition temperature, density and morphology of these defects for different doping levels. We will show that there appears to be a strong link between the line feature and superconductivity in these materials. We will discuss these questions from a crystallographic viewpoint.

4.1. Line defects and superconductivity

Structurally, the gallium compound is similar to YBCO in that the copper–oxygen chain is replaced by gallium–oxygen chains. Since the $CuO_{4/4}$ chain is missing, superconductivity in gallium materials implies a phenomenological interpretation that superconductivity in YBCO-type structures depends on interplane coupling to the double $CuO_{4/2}$, the conducting planes. A well known characteristic of YBCO is the orthogonal deformation of the copper–oxygen chains due to oxygen deficiency: T_c decreases with δ up to 0.7, and vanishes when b_p/a_p is less than 1% [13]. Here b_p and a_p are the dimensions of the perovskite unit viewed along the diagonal of the oxygen octahedron as illustrated in Fig. 6(a). In the undoped gallium compound, $YSr_2Cu_2GaO_7$, the two Ga–O chains in a unit are along the perovskite [110] direction with a glide-mirror plane perpendicular to the $(CuO_{4/2})$ plane, which results in a non-centersymmetrical structure and the angle between a_p and b_p as 0.9° off a right angle, but a_p and b_p remain the same, see Fig. 6(b). In $YSr_{2-x}Ca_xCu_2GaO_7$, X-ray and electron-diffraction studies show that the Ca substitution occupies the strontium sites homogeneously. As shown in Fig. 2(c), Ca substitution does not result in any defects in structure, and $a_p = b_p$. However, in $Y_{1-x}Ca_xSr_2Cu_2GaO_7$ where superconductivity is observed, Ca substitution for Y induced line features which are associated with a distortion of the gallium–oxygen planes. The line defects are incommensurate with the lattice, and can be detected in the [021] zone,

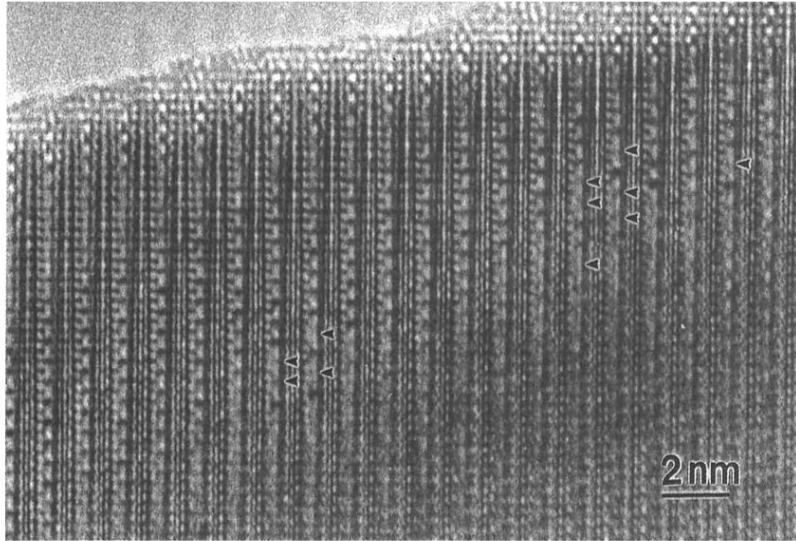


Fig. 5. High-resolution image along [001] where the line defects could be detected in some SrO–GaO–SrO layers as arrowed.

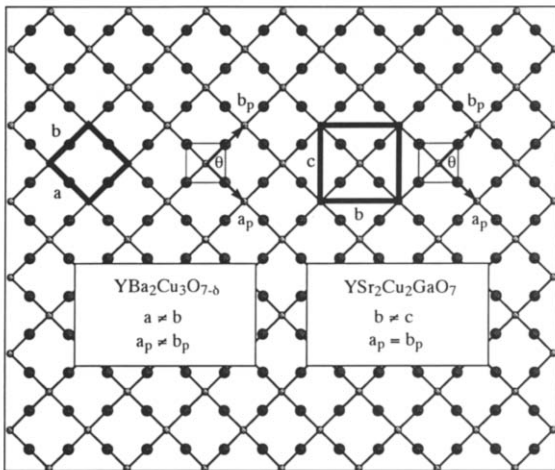


Fig. 6. The two Cu–O₂ half octahedra are deformed in different ways: (a) $a_p \neq b_p$ but $a_p \perp b_p$ in $\text{YBa}_2\text{Cu}_3\text{O}_{7-\delta}$; (b) $a_p = b_p$ but $\langle a_p, b_p \rangle \approx 89^\circ$ in $\text{YSr}_2\text{Cu}_2\text{GaO}_7$.

but not in [012]. This asymmetrical distortion leads to $a_p \neq b_p$.

4.2. Density of the line defects and the Meissner fraction

It has been found by X-ray diffraction that there is a lattice contraction of the Cu–O₂ planes in $\text{Y}_{1-x}\text{Ca}_x\text{Sr}_2\text{Cu}_2\text{GaO}_7$ as the calcium doping increases from $x=0$ to 0.4. Let us hypothesize that there is a

correlation between these defects and this lattice contraction, and then test this hypothesis. We measured the local periodicity along [012] of the defects relative to the matrix from a typical [021] pattern of $\text{Y}_{1-x}\text{Ca}_x\text{Sr}_2\text{Cu}_2\text{GaO}_7$ with $x=0.2$, as shown in Fig. 7. The distance of the streaks to the corresponding diffraction spots gives the ratio of the tubes to the lattice.

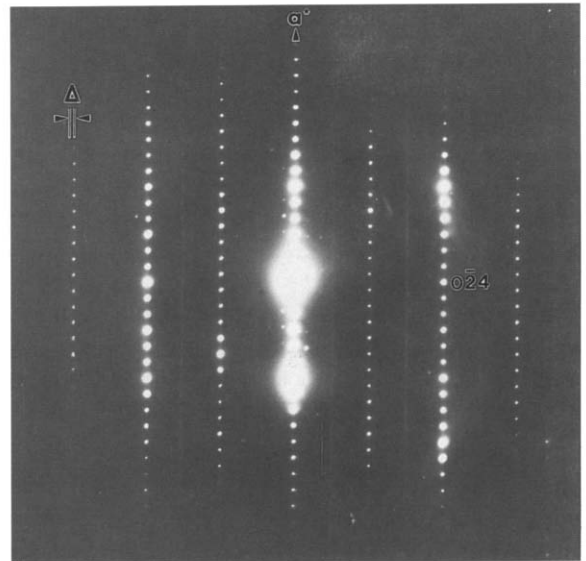


Fig. 7. A typical [021] pattern from $\text{Y}_{0.8}\text{Ca}_{0.2}\text{Sr}_2\text{Cu}_2\text{GaO}_7$ showing that the line defects are contracted compared with the lattice, since the streaks (arrowed) are located off the bulk diffraction spots.

It was measured from Fig. 7 that the tubes are 1.5% smaller along [012]. From the X-ray data [9], we knew that the *b* and *c*-axis were reduced by 0.09% and 0.11%, respectively, when the doping changed from $x = 0.0$ to 0.4, which means a contraction of about 0.3% along [012]. If we consider that about 20% of the strain is transmitted to the matrix, the X-ray results can be rationalized. It is interesting that the number 20% is close to the Meissner fraction, 15–18% in $x = 0.4$ materials, from SQUID measurements. This seems to imply that:

- (1) the contraction of the Cu–O₂ plane is due to the presence of the line defects;
- (2) at higher densities of the line defects there is a higher superconducting fraction.

4.3. Defect morphology and the transition temperature

The line defects show different morphologies at different calcium doping levels: lines at $x = 0.2$ with $T_c = 26$ K, and 8 Å/11 Å tubes at $x = 0.35$ with $T_c = 40$ K and $x = 0.4$ with $T_c = 44$ K samples. Our observations indicate that the 11 Å tubes are the major features in the gallium materials with the higher T_c 's. Our interpretation is that the different defective structures cause the geometry of the conducting plane to change ($a_p \neq b_p$).

4.4. Charge or internal pressure?

There are two partially competing views as to the structural role of the additional elements in the high-temperature superconductors. One approach is that they are to a large extent charge reservoirs, and doping of these materials changes the electronic structure of the copper–oxide planes. An alternative view is that the framework around the planes forces the correct spacings for a superconducting state. It is appropriate here to point out that the data on these gallium superconductors appears to strongly favor the second view. It is necessary to treat these compounds at high pressures in oxygen in order to produce the superconductor. This does not seem to alter the oxygen content, but does lead to a high concentration of line or tube defects. These have a smaller periodicity as mentioned above, and their formation will therefore be enhanced by a high-pressure treatment. An interpretation is that the high-

pressure oxygen synthesis mainly serves to prevent reduction of the compound, and the lattice contraction generated by the line defects removes sufficient charge from the antibonding orbitals to produce superconductivity.

5. Conclusion

Studies of the microstructure of Ca doped YSr₂Cu₂GaO₇ demonstrate that line defects are unique features of the Y_{1-x}Ca_xSr₂Cu₂GaO₇ superconductors, which are not observed in non-superconducting YSr_{2-x}Ca_xCu₂GaO₇, while both compounds have the same structure as YSr₂Cu₂GaO₇. The transition temperature and Meissner fraction increases with the doping level as does the defect structure and concentration, indicating a link between these defects and superconductivity in these materials. The line defects modify the symmetry of the gallium–oxygen chain which plays a similar role to the copper–oxygen chains in YBa₂Cu₃O_{7-δ}.

Acknowledgement

This work was supported by the Science and Technology Center for Superconductivity on grant number NSF/DMR-9120000.

References

- [1] K. Kishio, K. Kitazama, N. Suggii, S. Kanbe, K. Fueki, H. Takagi and S. Tanaka, *Chem. Lett.* (1987) 429.
- [2] (a) Y. Tokura, H. Takagi and S. Uchida, *Nature* (London) 337 (1989) 345;
(b) Y. Hidaka and M. Suzuki, *Nature* (London) 338 (1989) 635.
- [3] (a) R.J. Cava, B. Batlogg, R.B. van Dover, D.W. Murphy, S. Sunshine, T. Siegrist, J.P. Remeka, E.A. Rietman, S. Zahurak and G.P. Espinosa, *Phys. Rev. Lett.* 58 (1987) 1676;
(b) M.A. Beno, L. Solderholm, D.W. Capone II, D.G. Hinks, J.D. Jorgenson, J.D. Grace, I.K. Schuller, C.U. Segre and K. Zhang, *Appl. Phys. Lett.* 51 (1987) 57.
- [4] C.W. Chu, J. Bechtold, L. Gao, P.H. Hor, Z.J. Huang, R.L. Meng, Y.Y. Sun, Y.Q. Wang and Y.Y. Xue, *Phys. Rev. Lett.* 60 (1988) 941.
- [5] C.C. Toradi, M.A. Subramanian, J.C. Calabrese, J. Gopalakrishnan, J.J. Morrissey, T.R. Askew, R.B. Flippen, U. Choudhry and A.W. Sleight, *Science* 240 (1988) 631.

- [6] J.T. Vaughey, J.P. Theil, E.F. Hasty, D.A. Groenke, C.L. Stern, K.R. Poeppelmeier, B. Dabrowski, D.G. Hinks and A.W. Mitchell, *Chem. Mater.* 3 (1991) 935.
- [7] G. Roth, P. Adelman, R. Knitter and T. Wolf, *J. Phys. (Paris)* I 1 (1991) 721.
- [8] B. Dabrowski, P. Radaelli, D.G. Hinks, A.W. Mitchell, J.T. Vaughey, D.A. Groenke and K.R. Poeppelmeier, *Physica C* 193 (1992) 63.
- [9] J.P. Zhang, D.A. Groenke, H. Zhang, D.I. DeLoach, B. Dabrowski, K.R. Poeppelmeier, V.P. Dravid and L.D. Marks, *Physica C* 202 (1992) 51.
- [10] T. Krekels, O. Milat, G. Van Tendeloo, S. Amelinckx, T.G.N. Babu, A.J. Wright and C. Greaves, *J. Sol. State, Chem.* 105 (1993) 313;
O. Milat, T. Krekels, G. van Tendeloo and S. Amelinckx, *J. Phys. I (Paris)* 3 (1993) 1219.
- [11] J.P. Zhang, D.A. Groenke, B. Dabrowski, K.R. Poeppelmeier and L.D. Marks, *Mater. Sci. Forum* 129 (1993) 139.
- [12] J.B. Wiley, M. Sabat, S.J. Hwu and K.R. Poeppelmeier, *J. Solid State Chem.* 87 (1990) 250.
- [13] R.J. Cava, B. Batlogg, A.P. Ramirez, D. Werder, C.H. Chen, E.A. Rietman and S.M. Zahurak, *Proc. MRS Symp.* 99 (1987).